Reconstruction of a neural network from a time series of firing rates

A. Pikovsky

Institute for Physics and Astronomy, University of Potsdam, Karl-Liebknecht-Strasse 24/25, 14476 Potsdam-Golm, Germany
and Department of Control Theory, Nizhni Novgorod State University, Gagarin Avenue 23, 606950 Nizhni Novgorod, Russia

(Received 3 April 2016; revised manuscript received 30 May 2016; published 20 June 2016)

Randomly coupled neural fields demonstrate irregular variation of firing rates, if the coupling is strong enough, as has been shown by Sompolinsky *et al.* [Phys. Rev. Lett. **61**, 259 (1988)]. We present a method for reconstruction of the coupling matrix from a time series of irregular firing rates. The approach is based on the particular property of the nonlinearity in the coupling, as the latter is determined by a sigmoidal gain function. We demonstrate that for a large enough data set and a small measurement noise, the method gives an accurate estimation of the coupling matrix and of other parameters of the system, including the gain function.

DOI: 10.1103/PhysRevE.93.062313

I. INTRODUCTION

Understanding connectivity of networks of coupled dynamical units is a general problem appearing not only in physics, but also in ecology, epidemiology, genetic regulation, and climate dynamics (see, e.g., Refs. [1]). A particularly important application field is neuroscience, where revealing brain connectivity is a hot topic of current interest [2]. A general goal here is to reconstruct interactions between the nodes based on the observations of neurophysiological signals, e.g., on multichannel EEG or MEG measurements (see Refs. [3] and recent review [4]).

Many methods developed here are based on cross-correlations and mutual information analysis, applicable to general stochastic processes [5]. However, if the data belongs to a special class of processes with a known structure of the dynamical laws, much better reconstruction of connectivity can be achieved by virtue of special methods developed for this specific class. For example, if the signal sources can be considered as self-sustained oscillating units, powerful methods of analysis based on the phase dynamics equations have been developed [6].

In this paper we suggest a method for network reconstruction under the assumption that the observed irregular neural fields are firing rates, interacting according to a widely accepted model for the neural field dynamics (see Sec. II). We stress that in this paper we refer to the fields resulting from numerical simulations rather than generated experimentally. Each field is influenced by many others, which makes the problem of reconstruction nontrivial. On the other hand, the local dynamics is governed by a scalar differential equation, the structure of which is rather simple, which makes the whole problem tractable. Below we assume only knowledge of a general structure of the underlying dynamical equations, but not of their particular details; thus, our approach generalizes that of Ref. [7], where knowledge of the functions determining the dynamics has been assumed. Our method is analogous to the approach used to reconstruct a network of time-delayed units, suggested and applied to experimental data in Ref. [8].

The paper is organized as follows. We introduce the neural network model and demonstrate its chaotic behavior in Sec. II. The method for reconstruction of the connectivity and its application to the network introduced in Sec. II is described in Sec. III. Further possible extensions are discussed in the Conclusion.

II. NEURAL NETWORK MODEL AND ITS DYNAMICS

In this paper we focus on the reconstruction of the network structure that governs neural fields in the firing rates formulation, which is one of the basic models in computational neuroscience (see Refs. [9]; here we particularly follow Ref. [10]). Each of n nodes is characterized by its time-dependent firing rate $x_j(t)$, which evolves depending on inputs from other nodes according to a system of ordinary differential equations:

$$\tau_j \frac{dx_j}{dt} + x_j = F_j\left(\sum_{k=1}^{n} w_{jk}x_k\right), \quad j = 1,\ldots,n\,. \qquad (1)$$

Here τ_j is the time constant of relaxation of the field at node j, and F_j are gain functions at the nodes. The network is determined by the $n\times n$ coupling matrix w_{jk}. As has been shown in Ref. [11], at large enough coupling such a network demonstrates chaos, and this is a state that allows for reconstruction of the network matrix w_{jk} from the observations $x_j(t)$, as described below. We stress here that the concept of deterministic chaos is important in the context of a fully deterministic model Eq. (1) because here chaos ensures enough variability of the fields $x_j(t)$, in contradistinction to regular states like periodic orbits and steady states, where reconstruction will not work. In fact, what is needed is a sufficient degree of irregularity and variability of the fields to explore different states as described below. On the other hand, a sufficient degree of determinism is also needed, as the method is based on the assumption of validity of Eqs. (1).

We illustrate a chaotic state for the following set of parameters: $n = 100$; $1-\tau^0 < \tau_j < 1+\tau^0$ are random numbers taken from a uniform distribution with $\tau^0 = 0.1$. Functions F_j have the same form but different amplitudes: $F_j(u) = \alpha_j/[1+\exp(-u-\rho_j)]$, where $1-\alpha^0 < \alpha_j < 1+\alpha^0$ are random numbers taken from a uniform distribution with $\alpha^0 = 0.1$. The links w_{ij} are nonzero with probability $p_c = 0.15$ (thus, the connections are relatively sparse); their values are taken from a normal distribution $w_{ij} = JN(0,1)$ with $J = 8$. Finally, $\rho_i = \eta_i - 0.5\sum_j w_{ij}$, where η_i is taken from a normal distribution

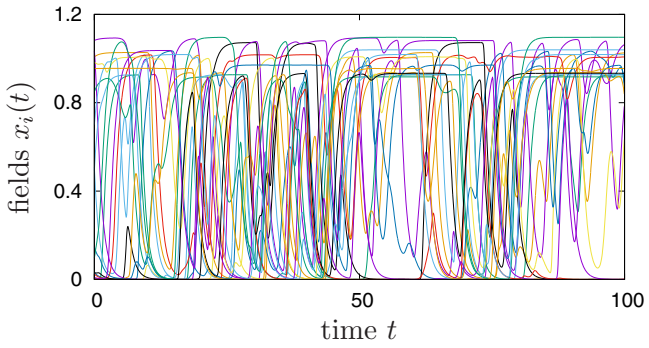

FIG. 1. Example of chaotic neural fields (first 20 fields $x_i(t)$, for $i = 1,\ldots,20$ are depicted with different colors).

$N(0,1)$. Figure 1 shows the first 20 chaotic fields $x_j(t)$, for a realization of parameters. This chaotic state is used below for illustration of the reconstruction method.

III. RECONSTRUCTION OF THE CONNECTIVITY MATRIX

A. Method of reconstruction

Suppose one observes the time series of all variables $\vec{x}(t)$ governed by Eq. (1). The problem is to reconstruct the coupling matrix w from these observations. We notice that the functions F_j and parameters τ_j are unknown and are generally different. We will see that the reconstruction method allows one to reveal these quantities as well.

The main idea is to use the monotonicity of the functions F, which we do not need to know explicitly. For illustration and to simplify notations, we discuss below only reconstruction of the function F_1, of the parameter τ_1, and of the coupling constants w_{1j}, all other quantities can be similarly determined. We denote the row of the coupling constants as a vector $\vec{c}$, where $c_j = w_{1j}$.

Suppose first that parameter τ_1 is known. Let us select all those points from the time series, for which $\tau_1\dot{x}_1 + x_1$ lies in a small neighborhood of a given value y. Let us denote the corresponding times as $t_1, t_2, \ldots, t_{m+1}$. Let us take vectors $\vec{x}(t_k)$, $k = 1,\ldots,m+1$ at these moments of time. Then, for all these vectors,

$$F_1[\vec{c}\cdot\vec{x}(t_k)] \approx y.$$

This means, because function F_1 is bijective, that

$$\vec{c}\cdot\vec{x}(t_k) \approx \vec{c}\cdot\vec{x}(t_j) \quad \text{for all} \quad k,j. \tag{2}$$

Therefore, for all pairs of indices j,k we have

$$\vec{c}\cdot[\vec{x}(t_k) - \vec{x}(t_j)] \approx 0. \tag{3}$$

However, these relations are not independent, because from $\vec{c}\cdot[\vec{x}(t_k) - \vec{x}(t_j)] \approx 0$ and $\vec{c}\cdot[\vec{x}(t_k) - \vec{x}(t_l)] \approx 0$ follows that $\vec{c}\cdot[\vec{x}(t_l) - \vec{x}(t_j)] \approx 0$. Thus, we need a set of relations, where each vector $\vec{x}(t_j)$ enters only twice. The simplest way to accomplish this is to define differences:

$$\vec{z}(k) = \vec{x}(t_{k+1}) - \vec{x}(t_k), \quad k = 1,\ldots,m.$$

In terms of these vectors we can rewrite Eq. (3) as

$$\vec{z}(k)\cdot\vec{c} = 0. \tag{4}$$

We need to find $\vec{c}$ from this set of equations. One can see that system Eq. (4) does not depend on the choice of y, thus we can take all possible observed values of y and obtain a large set of M vectors $\vec{z}$ that satisfy Eq. (4). This whole set should be used for determining the unknown coupling vector $\vec{c}$.

The formulated task is nothing more than solving homogeneous linear equations using singular value decomposition (SVD); see, e.g., Ref. [12]. The problem reduces to finding the null space of a $M\times n$ matrix A, composed of M vectors $\vec{z}(k)$ as the rows. Once the zero singular value of A is found, the corresponding entry in the obtained unitary matrix gives the vector $\vec{c}$ (up to a normalization, which anyhow cannot be found by this method because the function F_1 is unknown).

Above, we have assumed that the parameter τ_1 is given. In a realistic situation, however, parameter τ_1 is unknown. In this instance, the procedure above can be used for a set of values of τ_1, chosen from a reasonable, constrained range. For each such value the minimal singular value of matrix A can be found, and the proper τ_1 should be chosen as one yielding the minimum of these singular values.

The method described above is based on the simple observation that close values of the function F_1 mean that the arguments of this function are also close to each other. However, typically function F_1 is a sigmoidal function [in models often $\tanh(\cdot)$ is used], which has domains with the derivative close to zero, where the inversion is nearly singular. Therefore, the values of $y = \tau_1\dot{x}_1 + x_1$, which are nearly constants should be excluded from the analysis. Practically, we use all the points for which $|\dot{y}| > \sigma$, with some threshold σ. After all these points were extracted from a time series, the results were sorted. In this way, the nearest neighbors post sorting are the closest points for which $y(t_1) \approx y(t_2)$, and the corresponding difference vector $\vec{z} = \vec{x}(t_1) - \vec{x}(t_2)$ can then be used to fill the matrix A.

B. Numerical results

Here we present the results of the reconstruction of coupling, for the chaotic regime presented in Fig. 1. Figure 2

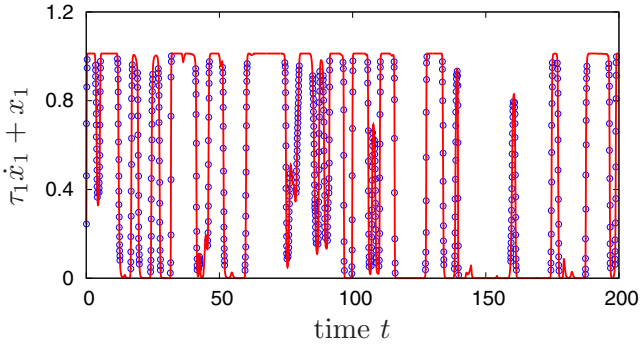

FIG. 2. Solid red line: $y(t) = \tau_1\dot{x}_1 + x_1$ is sampled with time step 0.05, points where $|\dot{y}| > 0.3$ are shown with blue circles. One can see that selection of relatively rapidly varying parts of the time series allows one to avoid nonsensitive epochs where the field $y(t)$ is nearly constant.

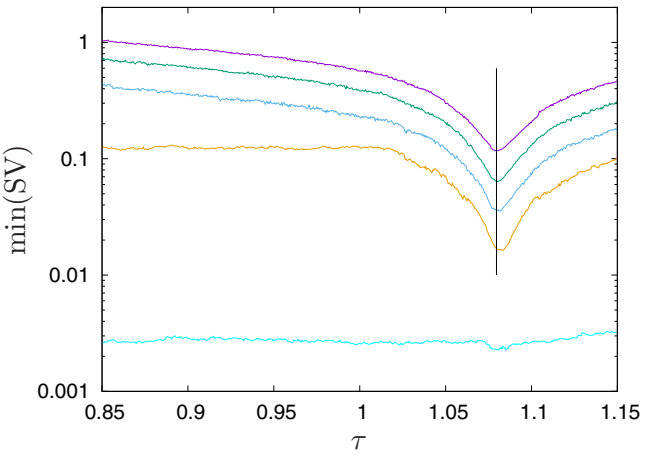

FIG. 3. Dependence of the minimal singular value on the parameter τ for different lengths of time series (from top to bottom: total used time intervals 2500,1250,500,250,100). The vertical line shows the true value of τ.

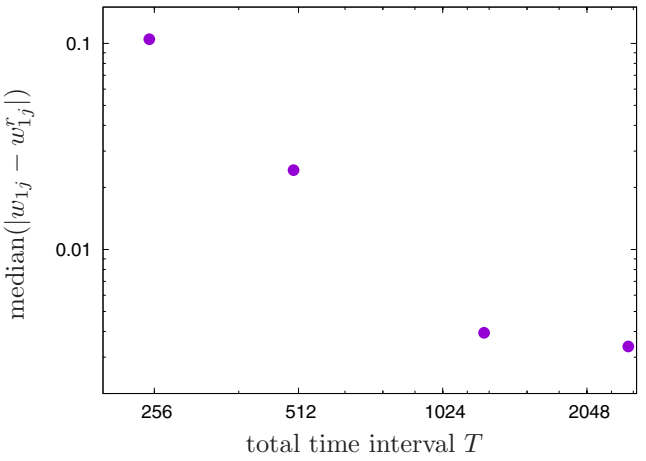

FIG. 5. Median errors for the reconstruction depicted in Fig. 4, as functions of the total time interval used.

illustrates the role of parameter σ that discriminates tails of function F_1 where its derivative is minimal. One can see that taking $\sigma = 0.3$ yields points in the bulk of the chaotic variations.

In Fig. 3 we show the results of calculations of the minimal singular value for the process presented in Fig. 2 with $\sigma = 0.3$, versus the test values of τ_1, for different total lengths of the time series. One can see that for the method to work, the length of the time series T should be large enough (in our case $T \gtrsim 250$)—otherwise the set of vectors $\vec{z}$ is too small and the distances between the neighbors of the sorted array of values of y are too large.

Based on the analysis presented in Fig. 3, in Fig. 4 we show the results of the reconstruction of the coupling coefficients [13], for four lengths of the time series used, that demonstrate a pronounced minimum of the singular value. The value of τ was taken from the corresponding minima. In all cases, the reconstructed coupling nearly coincides with the true one. This proves that the accuracy of the method is good, and it allows one to infer the connectivity matrix from the time series.

In Fig. 4, one can hardly distinguish the markers as they practically overlap. We have intentionally chosen this presentation to demonstrate how small are the errors compared to the characteristic values of the coupling constants. To characterize the accuracy in more detail, we calculated the medians of the distributions of errors $|w_{1j} - w^r_{1j}|$, where w_{1j} are coupling constants used in the simulations (they are shown with circles in Fig. 4), and w^r_{1j} are reconstructed values. One can see from Fig. 5 that, as expected, the accuracy is improved if a longer time series is available.

Finally, we show in Fig. 6 how the function F_1 is reconstructed after the coupling constants are found.

To check the robustness of the method, we studied how measurement noise influences the quality of the reconstruction. To this end, we added independent Gaussian random variables

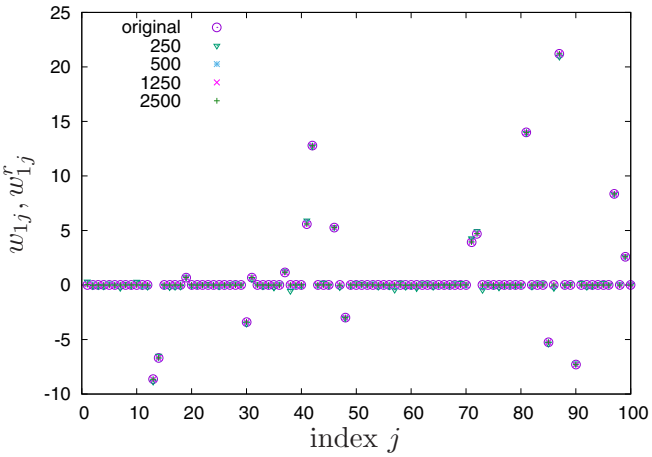

FIG. 4. Original coupling constants w_{1j} (circles) and the reconstructed ones w^r_{1j} for the data sets with total used time intervals $T = 2500,1250,500,250$ (the corresponding markers). In these sets the number of data points used for reconstruction was 8961,4174,1627,796, respectively.

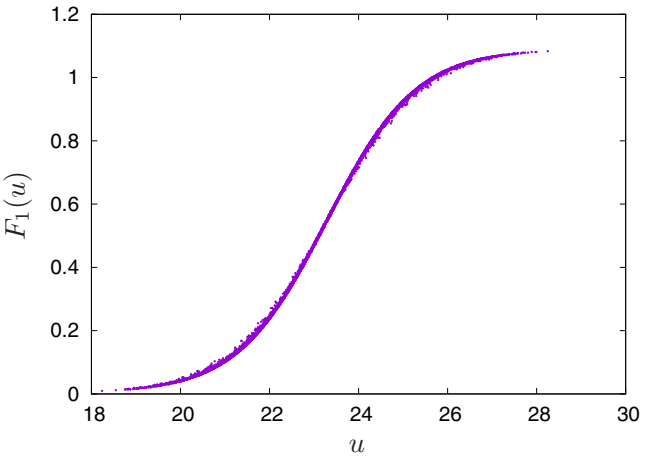

FIG. 6. Reconstruction of the gain function F_1. The same data points as in finding the coupling matrix Fig. 4, with $T = 2500$, are used. Points depict values of $\tau_1\dot{x}_1 + x_1$ versus $\sum_k w_{1k}x_k$ at all recorded time instants, where w_{1k} are the reconstructed coupling constants.

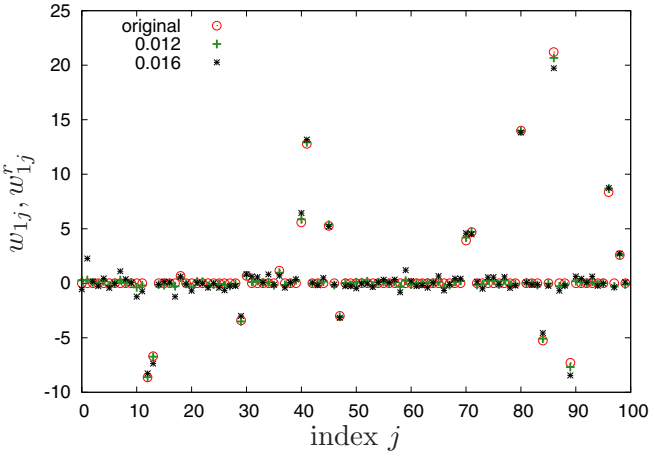

FIG. 7. Original coupling constants w_{1j} (circles) and the reconstructed ones w^r_{1j} for the data sets with total used time interval $T = 5000$, for two values of noise intensity: $\delta = 0.012$ and $\delta = 0.016$. The noisy data sets have been preprocessed with the Savitzky-Golay filter of order (16, 16, 4) (see Ref. [14]), the same filter has been used to calculate the derivatives.

with variance δ^2 to the same time series as used in Fig. 4. The results of the reconstruction for two noise intensities, shown in Fig. 7, should be compared with the noise-free case in Fig. 4. One can see that the reconstruction definitely worsens if the noise amplitude exceeds approximately 1.5% of that of the signal. Below this value, the quality of the reconstruction is pretty good.

IV. CONCLUSIONS

In summary, we have developed a method to reconstruct the connection network behind a collection of interacting neural fields, provided the observations of the firing rates on the nodes are available. The method delivers the connectivity matrix, together with the parameters characterizing the node's dynamics, such as the time constant and the gain function at each node. We have demonstrated that for a reliable reconstruction, a sufficient length of the time series and low measurement noise are needed. In this first study we assumed a rather ideal situation where data for all nodes are available and the dynamics is purely deterministic; exploration of the restrictions imposed by these assumptions is a subject of ongoing research.

We have formulated the method for the neural field model based on firing rates. There is an equivalent voltage formulation of the model where, in fact, other variables are used [10]. The approach described is not directly suited for these variables; its corresponding generalization remains a challenging task.

ACKNOWLEDGMENTS

We acknowledge useful discussions with V. Ponomarenko, Z. Levnajic, A. Daffertshofer, and M. Rosenblum. The work was supported by ITN COSMOS (funded by the European Unions Horizon 2020 research and innovation programme under the Marie Sklodowska-Curie Grant Agreement No. 642563) and by the Russian Science Foundation (analysis of the effect of noise, Project No. 14-12-00811).

[1] J. I. Deza, M. Barreiro, and C. Masoller, Chaos **25**, 033105 (2015); G. Sugihara, R. May, H. Ye, C.-h. Hsieh, E. Deyle, M. Fogarty, and S. Munch, Science **338**, 496 (2012); I. Tomovski and L. Kocarev, Phys. A: Stat. Mech. Appl. **436**, 272 (2015); Z. Li, P. Li, A. Krishnan, and J. Liu, Bioinformatics **27**, 2686 (2011).

[2] M. Boly, M. Massimini, M. Garrido, O. Gosseries, Q. Noirhomme, S. Laureys, and A. Soddu, Brain Connect. **2**, 1 (2012); E. Pastrana, Nat. Meth. **10**, 481 (2013); O. Sporns, *ibid.* **10**, 491 (2013).

[3] D. Smirnov, B. Schelter, M. Winterhalder, and J. Timmer, Chaos **17**, 013111 (2007); P. Skudlarski, K. Jagannathan, V. D. Calhoun, M. Hampson, B. A. Skudlarska, and G. Pearlson, NeuroImage **43**, 554 (2008); D. Chicharro, R. Andrzejak, and A. Ledberg, BMC Neurosci. **12**, P192 (2011); D. Yu and U. Parlitz, PLoS ONE **6**, e24333 (2011).

[4] K. Lehnertz, Physiol. Meas. **32**, 1715 (2011).

[5] B. Schelter, J. Timmer, and M. Eichler, J. Neurosci. Meth. **179**, 121 (2009); R. G. Andrzejak and T. Kreuz, Europhys. Lett. **96**, 50012 (2011); N. Rubido, A. C. Martí, E. Bianco-Martínez, C. Grebogi, M. S. Baptista, and C. Masoller, New J. Phys. **16**, 093010 (2014); G. Tirabassi, R. Sevilla-Escoboza, J. M. Buldú, and C. Masoller, Sci. Rep. **5**, 10829 (2015).

[6] B. Kralemann, A. Pikovsky, and M. Rosenblum, Chaos **21**, 025104 (2011); New J. Phys. **16**, 085013 (2014).

[7] Z. Levnajić and A. Pikovsky, Sci. Rep. **4**, 5030 (2014).

[8] I. V. Sysoev, M. D. Prokhorov, V. I. Ponomarenko, and B. P. Bezruchko, Phys. Rev. E **89**, 062911 (2014).

[9] F. C. Hoppensteadt and E. M. Izhikevich, *Weakly Connected Neural Networks* (Springer, Berlin, 1997); P. C. Bressloff, J. Phys. A: Math. Theoret. **45**, 033001 (2012).

[10] G. B. Ermentrout and D. H. Terman, in *Mathematical Foundations of Neuroscience*, Interdisciplinary Applied Mathematics, Vol. 35 (Springer, New York, 2010), pp. xvi+422.

[11] H. Sompolinsky, A. Crisanti, and H. J. Sommers, Phys. Rev. Lett. **61**, 259 (1988).

[12] L. N. Trefethen and D. Bau, III, in *Numerical Linear Algebra* (SIAM, Philadelphia, PA, 1997), pp. xii+361.

[13] Although only relative values of the coupling constants can be reconstructed, here for clarity of comparison we normalized them by the norm of true coupling vector $|\vec{c}|$.

[14] W. H. Press, S. T. Teukolsky, W. T. Vetterling, and B. P. Flannery, *Numerical Recipes in C: the Art of Scientific Computing*, 2nd ed. (Cambridge University Press, Cambridge, England, 1992).